Novel Cholesteric Glassy Liquid Crystals Comprising Benzene Functionalized with Hybrid Chiral-Nematic Mesogens

Chunki Kim, Kenneth L. Marshall, Jason U. Wallace, Jane J. Ou, and Shaw H. Chen*

Department of Chemical Engineering, University of Rochester, Rochester, New York 14623-1212, and Laboratory for Laser Energetics, 250 East River Road, University of Rochester, Rochester, New York 14627-0166

Received June 14, 2008. Revised Manuscript Received July 13, 2008

With 4′-cyanobiphenyl-4-yl benzoate nematogens chemically bonded to a benzene core via enantiomeric 2-methylpropyl spacers, a new series of cholesteric glassy liquid crystals has been synthesized for an investigation of structure−property relationships. Glass-forming ability, phase-transition temperatures, and stability against crystallization are affected by both the number and the position of substituent groups on the benzene ring with 1,3,5-trisubstituted system possessing the most favorable set of properties, T_g at 73 °C and T_c at 295 °C. With (*S*)-3-bromo-2-methylpropanol as the chiral precursor, left-handed helical stacking was observed for all the cholesteric GLCs reported herein. Films of the 1,3,5-trisubstituted and meta-disubstituted systems show a selective reflection wavelength, λ_R, at 413 and 422 nm, respectively, whereas that of the ortho-isomer exhibits a λ_R at 860 nm. Replacing one of the hybrid chiral-nematic mesogen in the 1,3,5-trisubstituted system by a nematogen loosens the helical pitch to yield a λ_R at 630 nm, still shorter than that of the ortho-isomer despite the dilution by a nematogen. This observation suggests the importance of regioisomerism to helical twisting. The difference in λ_R was interpreted in terms of molecular packing involving chiral spacers through computational chemistry. The susceptibility of cholesteric GLCs to photoalignment was tested using the ortho-isomer. The degree of photoalignment improves with an increasing rotational mobility of pendant coumarin monomers to an extent comparable to mechanical alignment on conventional rubbed polyimide films.

Introduction

Liquid crystals are spontaneously ordered fluids characterized by a uniaxial, lamellar, helical, or columnar arrangement in nematic, smectic, cholesteric, or discotic mesophase, respectively. Preserving these molecular arrangements in the solid state via cooling through glass-transition temperature (T_g), glassy liquid crystals (GLCs) represent a unique material class potentially useful for organic optoelectronics. Whereas all liquids are expected to vitrify at a sufficiently rapid cooling rate, most organic materials, including liquid crystals, tend to crystallize upon cooling through the melting point, T_m. Crystallization of liquid crystals essentially destroys the desired molecular order that prevails in the fluid state, resulting in polycrystalline films that scatter light or impede charge transport. The very first attempt to synthesize GLCs in 1971 yielded materials with a low T_g and poor morphological stability,[1] namely, the tendency to crystallize on heating above T_g or cooling from T_m. Subsequent efforts have produced GLCs that can be categorized into (i) laterally or terminally branched, one-string compounds with a T_g mostly around room temperature;[2−4] (ii) twin molecules with an above-ambient T_g but generally lacking morphological stability;[5−8] (iii) cyclosiloxanes functionalized with mesogenic and chiral pendants;[9−13] (iv) carbosilane dendrimers exhibiting a low T_g;[14,15] (v) macrocarbocycles with mesogenic segments as part of the ring structure;[16] and (vi) Pentaerythritol as the central core to yield widely varying T_g and morphological stability.[17−20]

* To whom all correspondence should be addressed. E-mail: shch@lle.rochester.edu.

(1) (a) Tsuji, K.; Sorai, M.; Seki, S. *Bull. Chem. Soc. Jpn.* **1971**, *44*, 1452. (b) Sorai, M.; Seki, S. *Bull. Chem. Soc. Jpn.* **1971**, *44*, 2887.
(2) Wedler, W.; Demus, D.; Zaschke, H.; Mohr, K.; Schafer, W.; Weissflog, W. *J. Mater. Chem.* **1991**, *1*, 347.
(3) Loddoch, M.; Marowsky, G.; Schmid, H.; Heppke, G. *Appl. Phys. B: Laser Opt.* **1994**, *59*, 591.
(4) Rauch, S.; Selbmann, C.; Bault, P.; Sawade, H.; Heppke, G.; Morales-Saavedra, O.; Huang, M. Y.; Jákli, A. *Phys. Rev. E* **2004**, *69*, 021707.
(5) Attard, G. S.; Imrie, C. T. *Liq. Cryst.* **1992**, *11*, 785.
(6) Dehne, H.; Roger, A.; Demus, D.; Diele, S.; Kresse, H.; Pelzl, G.; Wedler, W.; Weissflog, W. *Liq. Cryst.* **1989**, *6*, 47.
(7) Attard, G. S.; Imrie, C. T.; Karasz, F. E. *Chem. Mater.* **1992**, *4*, 1246.
(8) Tamaoki, N.; Kruk, G.; Matsuda, H. *J. Mater. Chem.* **1999**, *9*, 2381.
(9) (a) Kreuzer, F. H.; Andrejewski, D.; Haas, W.; Haberle, N.; Riepl, G.; Spes, P. *Mol. Cryst. Liq. Cryst.* **1991**, *199*, 345. (b) Kreuzer, F. H.; Maurer, R.; Spes, P. *Makromol. Chem., Macromol. Symp.* **1991**, *50*, 215.
(10) Walba, D. M.; Zummach, D. A.; Wand, M. D.; Thurmes, W. N.; Moray, K. M.; Arnett, K. E. In *Liquid Crystal Materials, Devices, and Applications II*; Wand, M. D., Efron, U., Eds.; SPIE: San Jose, CA, 1993; Vol. 1911, p 21.
(11) Gresham, K. D.; McHugh, C. M.; Bunning, T. J.; Crane, R. J.; Klei, H. E.; Samulski, E. T. *J. Polym. Sci.: Part A: Polym. Chem.* **1994**, *32*, 2039.
(12) Saez, I. M.; Goodby, J. W.; Richardson, R. M. *Chem.—Eur. J.* **2001**, *7*, 2758.
(13) Saez, I. M.; Goodby, J. W. *J. Mater. Chem.* **2001**, *11*, 2845.
(14) Lorenz, K.; Hölter, D.; Stühn, B.; Mülhaupt, R.; Frey, H. *Adv. Mater.* **1996**, *8*, 414.
(15) Ponomarenko, S. A.; Boiko, N. I.; Shibaev, V. P.; Richardson, R. M.; Whitehouse, I. J.; Rebrov, E. A.; Muzafarov, A. M. *Macromolecules* **2000**, *33*, 5549.
(16) Percec, V.; Kawasumi, M.; Rinaldi, P. L.; Litman, V. E. *Macromolecules* **1992**, *25*, 3851.
(17) Van de Witte, P.; Lub, J. *Liq. Cryst.* **1999**, *26*, 1039.
(18) Pfeuffer, T.; Hanft, D.; Strohriegl, P. *Liq. Cryst.* **2002**, *29*, 1555.

10.1021/cm801623a CCC: $40.75
Published on Web 08/22/2008

Aiming at GLCs with elevated T_g and clearing point, T_c, accompanied by superior morphological stability, we have implemented a comprehensive molecular design strategy in which mesogenic and chiral pendants are chemically bonded to a finite volume-excluding core.[21−34] Although the core and pendant are crystalline as separate entities, the chemical hybrid with a proper flexible spacer connecting the two readily vitrifies into a GLC on cooling. A definitive set of GLCs has been synthesized and characterized to furnish insight into structure−property relationships and to demonstrate optical and photonic device concepts. In particular, cholesteric GLCs are potentially useful as large area nonabsorbing polarizers, optical notch filters and reflectors, and polarizing fluorescent films. Moreover, cholesteric GLC films can serve as a one-dimensional photonic bandgap for circularly polarized lasing.[35] Comprising separate chiral and nematic pendants, cholesteric GLCs have been synthesized either by a statistical approach, which requires intensive workup procedures to arrive at pure components,[26,36] or by deterministic approaches, which require long synthesis schemes.[22,37−39]

The present study was motivated to develop a new class of cholesteric glassy liquid crystals consisting of hybrid chiral-nematic mesogens, instead of separate chiral and nematic pendants, chemically bonded to a volume-excluding core. Previous attempts at hybrid chiral-nematic pendants have met with little or no success. For example, hybrid chiral-nematic pendants with a chiral tail yielded exclusively smectic mesomorphism,[40] and cyanotolan with a chiral spacer to a cyclohexane core failed to achieve mesomorphism.[21] To be practically useful, the targeted materials must possess elevated phase transition temperatures, stability against crystallization from the glassy state, and selective reflection across the visible to near-infrared region. With 4′-cyanobiphenyl-4-yl benzoate nematogens and enantiomeric 2-methylpropylene spacers connected to a benzene core, novel cholesteric GLCs have been synthesized for a systematic investigation of mesomorphic behavior, morphological stability, and optical properties as functions of molecular structure. In addition, a morphologically stable cholesteric GLC has been used to test its amenability to photoalignment on coumarin-containing polymer films that are capable of orienting a nematic fluid, E-7.[41−45]

Experimental Section

Material Synthesis. All chemicals, reagents, and solvents were used as received from commercial sources without further purification except tetrahydrofuran (THF) that had been distilled over sodium and benzophenone. The following intermediates were synthesized according to literature literatures: 1,3,5-benzenetricarboxylic acid, 1-tert-butyl ester,[38] 4-(3-hydroxypropoxy)benzoic acid 4′-cyanobiphenyl-4-yl ester (*Nm*−OH),[38] and 7-[4-[(3-hydroxypropoxy)benzoyloxy]coumarin.[44] Compounds **I**−**VIII** and polymer **C** for photoalignment, as depicted in Charts 1 and 2, were synthesized according to Schemes 1 and 2, respectively. Synthesis, purification, and characterization of polymers **A** and **B** have been reported previously,[44] and those for all the intermediates are included in the Supporting Information.

1,3,5-Benzenetricarboxylic Acid, tris[(*R*)-3-[(4′-Cyanobiphenyl-4-yl)oxy]-2-methylpropyl] Ester, I. To a solution of 1,3,5-benzenetricarboxylic acid (0.063 g, 0.30 mmol), *Ch*$_1$−OH (0.25 g, 0.94 mmol), and triphenylphosphine (TPP) (0.26 g, 1.0 mmol) in anhydrous tetrahydrofuran (3.1 mL) was added diethyl azodicarboxylate (DEADC) (0.19 g, 1.1 mmol) dropwise. The reaction was stirred under argon at room temperature overnight. The solvent was then removed under reduced pressure, and the solid residue was purified by gradient column chromatography on silica gel with 0−2% acetone in methylene chloride. The product was collected by precipitation from a methylene chloride solution into methanol to yield **I** (0.15 g, 53%). Anal. Calcd: C, 75.22; H, 5.37; N, 4.39. Found: C, 75.08; H, 5.53; N, 4.09. ^{1}H NMR spectral data (400 MHz, $CDCl_3$): δ 1.22 (d, 9H, $-CH_3$), 2.54 (m, 3H, $-CH_2CH(CH_3)CH_2-$), 4.04 (d, 6H, $-CH_2OAr$), 4.48 (m, 6H, $-COOCH_2-$), 7.01 (d, 6H, aromatics), 7.53 (d, 6H, aromatics), 7.64 (d, 6H, aromatics), 7.70 (d, 6H, aromatics), 8.87 (s, 3H, aromatics).

1,3,5-Benzenetricarboxylic Acid, tris[(*R*)-3-[4-[(4′-Cyanobiphenyl-4-yl)oxycarbonyl] phenoxy]-2-methylpropyl] Ester, II. The procedure for the synthesis of **I** was followed to prepare **II** using *Ch*$_2$−OH (0.41 g, 1.1 mmol) instead of *Ch*$_1$−OH in 66% yield (0.29 g). Anal. Calcd: C, 73.79; H, 4.82; N, 3.19. Found: C, 73.66; H, 4.65; N, 3.13. ^{1}H NMR spectral data (400 MHz, $CDCl_3$): δ 1.21 (d, 9H, $-CH_3$), 2.55 (m, 3H, $-CH_2CH(CH_3)CH_2-$), 4.06 (d, 6H, $-CH_2OAr$), 4.47 (m, 6H, $-COOCH_2-$), 6.98 (d, 6H,

(19) Yao, D.-S.; Zhang, B.-Y.; Li, Y.-H.; Xiao, W.-Q. *Tetrahedron Lett.* **2004**, *45*, 8953.
(20) Saez, I. M.; Goodby, J. W. *J. Mater. Chem.* **2003**, *13*, 2727.
(21) Shi, H.; Chen, S. H. *Liq. Cryst.* **1994**, *17*, 413.
(22) (a) Shi, H.; Chen, S. H. *Liq. Cryst.* **1995**, *18*, 733. (b) Shi, H.; Chen, S. H. *Liq. Cryst.* **1995**, *19*, 849.
(23) Mastrangelo, J. C.; Blanton, T. N.; Chen, S. H. *Appl. Phys. Lett.* **1995**, *66*, 2212.
(24) Shi, H.; Chen, S. H. *Liq. Cryst.* **1995**, *19*, 785.
(25) Chen, S. H.; Mastrangelo, J. C.; Shi, H.; Bashir-Hashemi, A.; Li, J.; Gelber, N. *Macromolecules* **1995**, *28*, 7775.
(26) (a) Chen, S. H.; Jin, R. J.; Katsis, D.; Mastrangelo, J. C.; Papernov, S.; Schmid, A. W. *Liq. Cryst.* **2000**, *27*, 201. (b) Fan, F. Y.; Mastrangelo, J. C.; Katsis, D.; Blanton, T. *Liq. Cryst.* **2000**, *27*, 1239.
(27) De Rosa, M. E.; Adams, W. W.; Bunning, T. J.; Shi, H.; Chen, S. H. *Macromolecules* **1996**, *29*, 5650.
(28) Chen, S. H.; Mastrangelo, J. C.; Blanton, T. N.; Bashir-Hashemi, A. *Liq. Cryst.* **1996**, *21*, 683.
(29) Chen, S. H.; Shi, H.; Conger, B. M.; Mastrangelo, J. C.; Tsutsui, T. *Adv. Mater.* **1996**, *8*, 998.
(30) Chen, S. H.; Mastrangelo, J. C.; Blanton, T. N.; Bashir-Hashemi, A. *Macromolecules* **1997**, *30*, 93.
(31) Chen, S. H.; Katsis, D.; Mastrangelo, J. C.; Schmid, A. W.; Tsutsui, T.; Blanton, T. N. *Nature* **1999**, *397*, 506.
(32) Fan, F. Y.; Culligan, S. W.; Mastrangelo, J. C.; Katsis, D.; Chen, S. H.; Blanton, T. N. *Chem. Mater.* **2001**, *13*, 4584.
(33) Chen, S. H.; Mastrangelo, J. C.; Jin, R. J. *Adv. Mater.* **1999**, *11*, 1183.
(34) Chen, S. H.; Chen, H. M. P.; Geng, Y.; Jacobs, S. D.; Marshall, K. L.; Blanton, T. N. *Adv. Mater.* **2003**, *15*, 1061.
(35) Shibaev, P. V.; Kopp, V. I.; Genack, A. Z.; Hanelt, E. *Liq. Cryst.* **2003**, *30*, 1391.
(36) Katsis, D.; Chen, H. P.; Mastrangelo, J. C.; Chen, S. H.; Blanton, T. N. *Chem. Mater.* **1999**, *11*, 1590.
(37) Chen, H. P.; Katsis, D.; Mastrangelo, J. C.; Chen, S. H.; Jacobs, S. D.; Hood, P. J. *Adv. Mater.* **2000**, *12*, 1283.
(38) Chen, H. M. P.; Katsis, D.; Chen, S. H. *Chem. Mater.* **2003**, *15*, 2534.
(39) Wallace, J. U.; Chen, S. H. *Ind. Eng. Chem. Res.* **2006**, *45*, 4494.
(40) Delavier, P.; Etzbach, K.-H.; Schmidt, A. J.; Siemensmeyer, K.; Wagenblast, G. U.S. Patent, 5 804 097, 1998.
(41) Schadt, M.; Seiberle, H.; Schuster, A. *Nature* **1996**, *381*, 212.
(42) Obi, M.; Morino, S.; Ichimura, K. *Chem. Mater.* **1999**, *11*, 656.
(43) Jackson, P. O.; O'Neill, M.; Duffy, W. L.; Hindmarsh, P.; Kelly, S. M.; Owen, G. J. *Chem. Mater.* **2001**, *13*, 694.
(44) Kim, C.; Wallace, J. U.; Trajkovska, A.; Ou, J. J.; Chen, S. H. *Macromolecules* **2007**, *40*, 8924.
(45) Kim, C.; Trajkovska, A.; Wallace, J. U.; Chen, S. H. *Macromolecules* **2006**, *39*, 3817.

Chart 1. Molecular Structures of All the Cholesteric Liquid Crystals Synthesized for This Study with Their Phase Transition Temperatures Expressed in °C As Determined by DSC Thermograms[a]

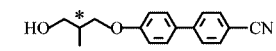

***Ch*$_1$–OH**: *G* –11 *Ch* (30 K_1 44 K_2) K_1 83 K_2 88 *I*
I 59 *Ch* ~–20 *G*

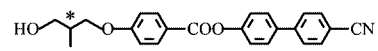

***Ch*$_2$–OH**: K_1 137 *Ch* 258 *I*
I 252 *Ch* 63 K_2 52 K_1

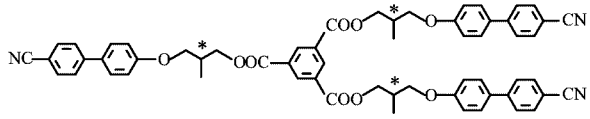

I: *G* 63 *I*

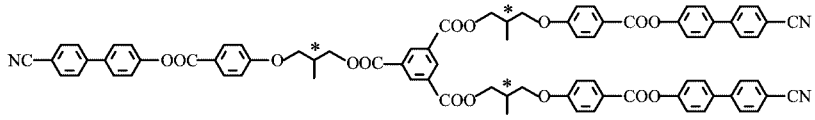

II: *G* 73 *Ch* 295 *I*

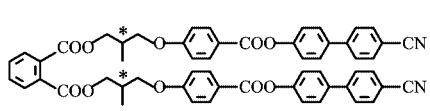

III: *G* 52 *Ch* 256 *I*

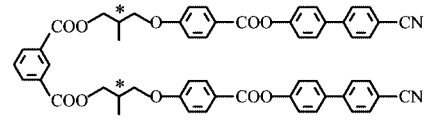

IV: *G* 52 *Ch* 275 *I*

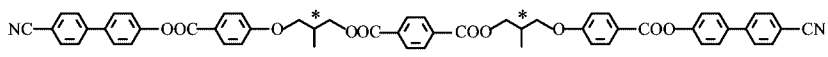

V: K_1 (156 K_2) 204 *Ch* 313 *I*
I 308 *Ch* 110 K_1

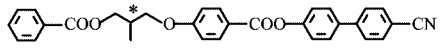

VI: K_1 23 K_2 32 K_3 (53 K_4 65 K_5) 112 *Ch* 192
I 187 *Ch* 27 K_1

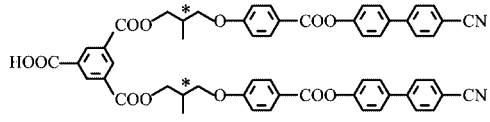

VII: *G* 87 *Ch* 271 *I*

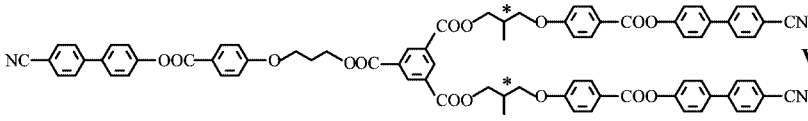

VIII: *G* 74 *Ch* 314 *I*

[a] Heating and cooling scans are reported as first and second line, respectively, and only the heating scans are reported for morphologically stable compounds. Symbols: *G*, glassy; *K*, crystalline; *Ch*, cholesteric; *I*, isotropic.

Chart 2. Chemical Structures of Coumarin-Containing Polymers A, B, and C for Photoalignment of Cholesteric GLC Films

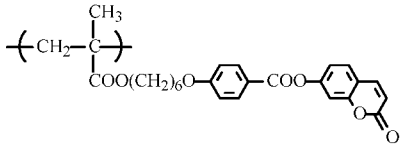

Polymer A: T_g = 68°C
$\overline{M}_w$ = 76,300 g/mol; $\overline{M}_w/\overline{M}_n$ = 3.3

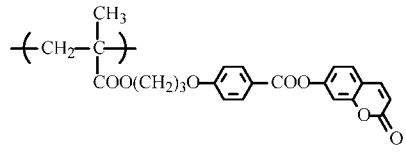

Polymer B: T_g = 102°C
$\overline{M}_w$ = 58,000 g/mol; $\overline{M}_w/\overline{M}_n$ = 3.4

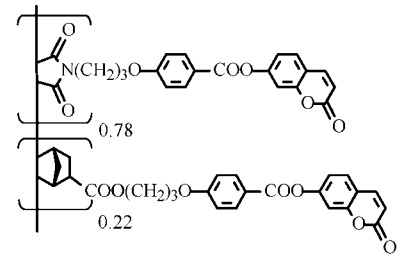

Polymer C: T_g = 135°C
$\overline{M}_w$ = 36,600 g/mol; $\overline{M}_w/\overline{M}_n$ = 2.1

aromatics), 7.29 (d, 6H, aromatics), 7.62 (d, 6H, aromatics), 7.66 (d, 6H, aromatics), 7.72 (d, 6H, aromatics), 8.14 (d, 6H, aromatics), 8.85 (d, 3H, aromatics).

1,2-Benzenedicarboxylic Acid, bis[(R)-3-[4-[(4′-Cyanobiphenyl-4-yl)oxycarbonyl]phenoxy]-2-methylpropyl] Ester, III. The procedure for the synthesis of **II** was followed to prepare **III** using

Scheme 1. Synthesis of *Ch*$_1$−OH, *Ch*$_2$−OH, and I−VIII without Altering Stereochemistry at the Asymmetric Carbon Center Inherited from (*S*)-3-Bromo-2-methylpropanol

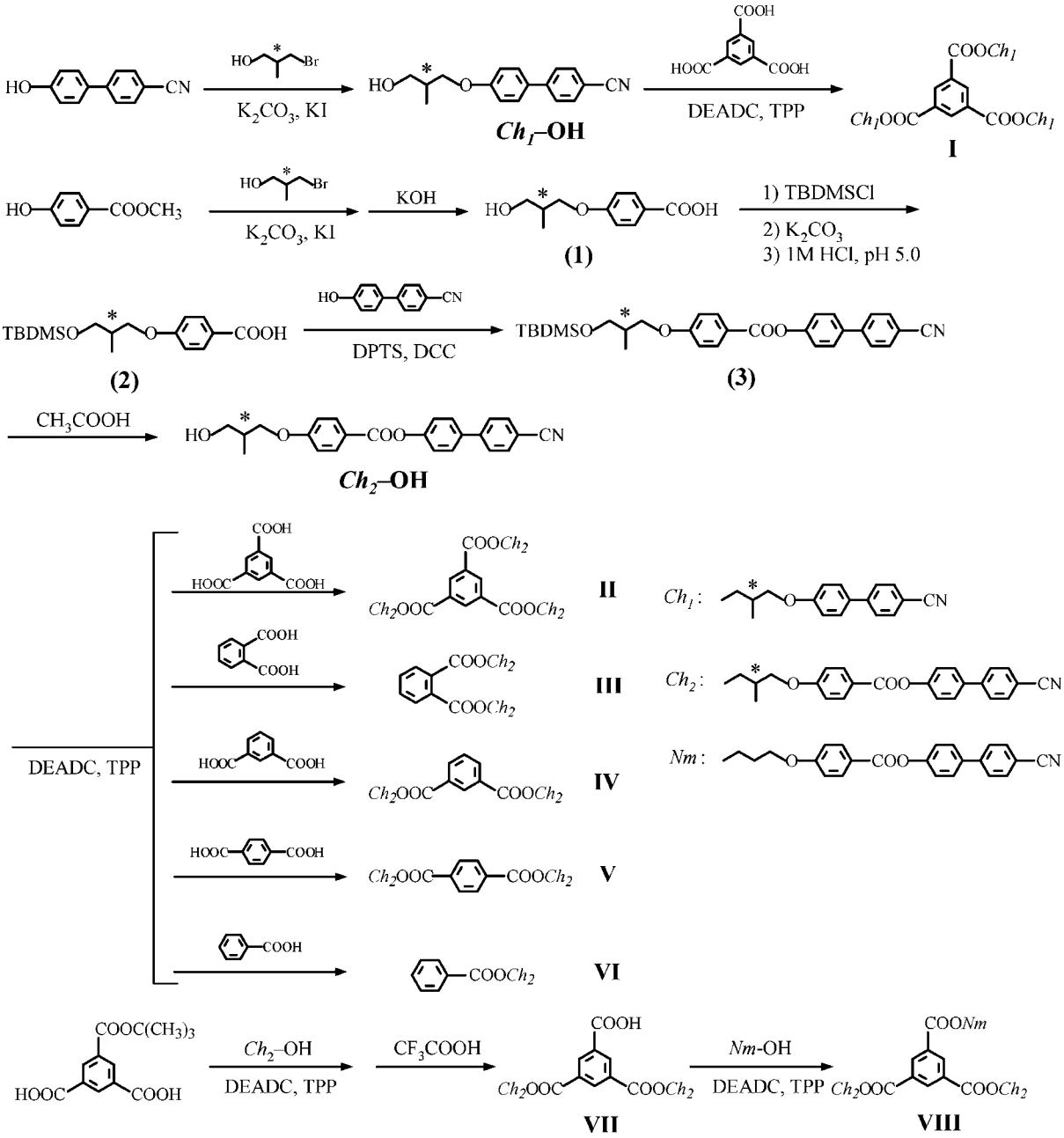

1,2-benzenedicarboxylic acid (0.031 g, 0.18 mmol) instead of 1,3,5-benzenetricarboxylic acid in 54% yield (0.090 g). Anal. Calcd: C, 74.32; H, 4.90; N, 3.10. Found: C, 73.90; H, 4.56; N, 3.04. ^{1}H NMR spectral data (400 MHz, $CDCl_3$): δ 1.15 (d, 6H, −C*H*$_3$), 2.45 (m, 2H, −CH$_2$C*H*(CH$_3$)CH$_2$−), 4.01 (m, 4H, −C*H*$_2$OAr), 4.35 (m, 4H, −COOC*H*$_2$−), 6.98 (d, 4H, aromatics), 7.29 (d, 4H, aromatics), 7.55 (m, 2H, aromatics), 7.61 (d, 4H, aromatics), 7.66 (d, 4H, aromatics), 7.71 (m, 6H, aromatics), 8.13 (d, 4H, aromatics).

1,3-Benzenedicarboxylic Acid, bis[(*R*)-3-[4-[(4′-Cyanobiphenyl-4-yl)oxycarbonyl]phenoxy]-2-methylpropyl] Ester, IV. The procedure for the synthesis of **II** was followed to prepare **IV** using 1,3-benzenedicarboxylic acid (0.031 g, 0.18 mmol) instead of 1,3,5-benzenetricarboxylic acid in 78% yield (0.13 g). Anal. Calcd: C, 74.32; H, 4.90; N, 3.10. Found: C, 74.08; H, 4.50; N, 3.03. ^{1}H NMR spectral data (400 MHz, $CDCl_3$): δ 1.21 (d, 6H, −C*H*$_3$), 2.54 (m, 2H, −CH$_2$C*H*(CH$_3$)CH$_2$−), 4.06 (m, 4H, −C*H*$_2$OAr), 4.45 (m, 4H, −COOC*H*$_2$−), 6.98 (d, 4H, aromatics), 7.30 (d, 4H, aromatics), 7.55 (t, 1H, aromatics), 7.62 (d, 4H, aromatics), 7.67 (d, 4H, aromatics), 7.72 (d, 4H, aromatics), 8.15 (d, 4H, aromatics), 8.23 (d, 2H, aromatics), 8.69 (s, 1H, aromatics).

1,4-Benzenedicarboxylic Acid, bis[(*R*)-3-[4-[(4′-Cyanobiphenyl-4-yl)oxycarbonyl]phenoxy]-2-methylpropyl] Ester, V. The procedure for the synthesis of **II** was followed to prepare **V** using 1,4-benzenedicarboxylic acid (0.031 g, 0.18 mmol) instead of 1,3,5-benzenetricarboxylic acid in 75% yield (0.13 g). Anal. Calcd: C, 74.32; H, 4.90; N, 3.10. Found: C, 73.95; H, 4.57; N, 3.07. ^{1}H NMR spectral data (400 MHz, $CDCl_3$): δ 1.21 (d, 6H, −C*H*$_3$), 2.55 (m, 2H, −CH$_2$C*H*(CH$_3$)CH$_2$−), 4.07 (m, 4H, −C*H*$_2$OAr), 4.45 (m, 4H, −COOC*H*$_2$−), 6.98 (d, 4H, aromatics), 7.31 (d, 4H, aromatics), 7.62 (d, 4H, aromatics), 7.67 (d, 4H, aromatics), 7.72 (d, 4H, aromatics), 8.10 (s, 4H, aromatics), 8.15 (d, 4H, aromatics).

Benzoic Acid [(*R*)-3-[4-[(4′-Cyanobiphenyl-4-yl)oxycarbonyl]phenoxy]-2-methylpropyl] Ester, VI. The procedure for the synthesis of **II** was followed to prepare **VI** using benzoic acid (0.029 g, 0.24 mmol) instead of 1,3,5-benzenetricarboxylic acid in 78% yield (0.090 g). Anal. Calcd: C, 75.75; H, 5.13; N, 2.85. Found: C,

Scheme 2. Synthesis of Coumarin-Containing Polymer C

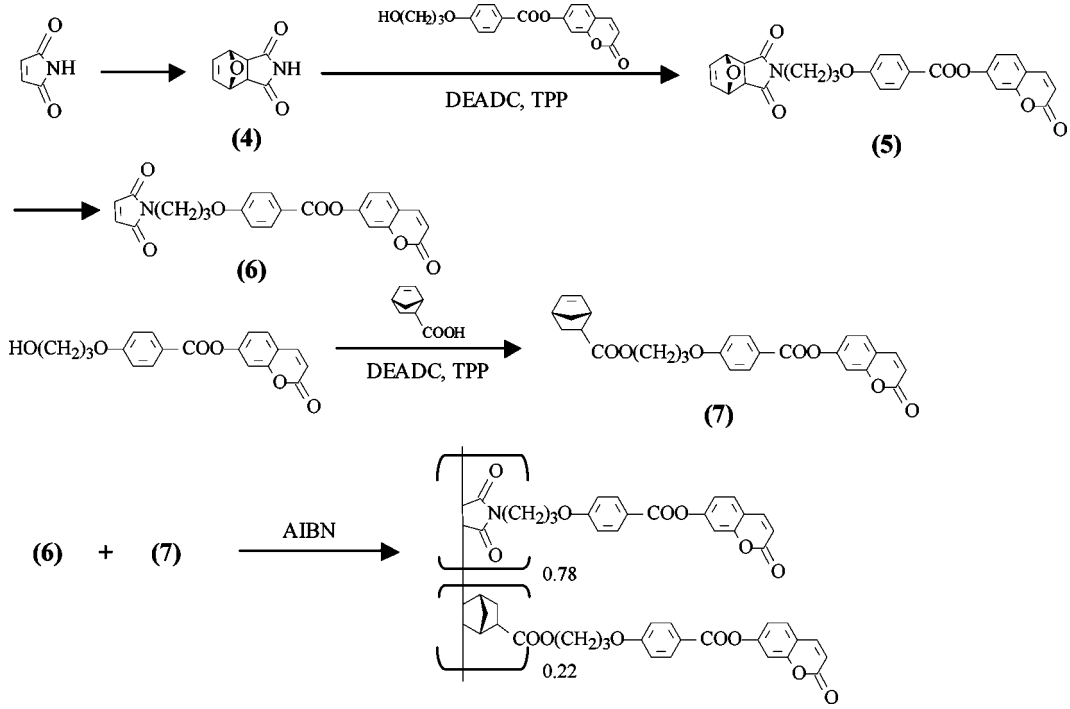

75.80; H, 4.86; N, 2.79. ^{1}H NMR spectral data (400 MHz, $CDCl_3$): δ 1.21 (d, 3H, $-CH_3$), 2.52 (m, 1H, $-CH_2CH(CH_3)CH_2-$), 4.08 (m, 2H, $-CH_2OAr$), 4.41 (m, 2H, $-COOCH_2-$), 6.99 (d, 2H, aromatics), 7.31 (d, 2H, aromatics), 7.46 (t, 2H, aromatics), 7.60 (t, 1H, aromatics), 7.63 (d, 2H, aromatics), 7.68 (d, 2H, aromatics), 7.73 (d, 2H, aromatics), 8.04 (d, 2H, aromatics), 8.15 (d, 2H, aromatics).

1,3,5-Benzenetricarboxylic Acid, 1,3-bis[(R)-3-[4-[(4′-Cyanobiphenyl-4-yl)oxycarbonyl] phenoxy]-2-methylpropyl] Ester, VII. To a solution of 1,3,5-benzenetricarboxylic acid, 1-*tert*-butyl ester (0.55 g, 2.1 mmol), Ch_2-OH (1.7 g, 4.3 mmol), and TPP (1.2 g, 4.5 mmol) in anhydrous tetrahydrofuran (35 mL) was added DEADC (0.79 g, 4.5 mmol) dropwise. The reaction mixture was stirred under argon at room temperature overnight. The solvent was removed under reduced pressure, and the crude product was purified by gradient column chromatography with 0−1% acetone in methylene chloride. The *tert*-butyl ester was hydrolyzed in anhydrous methylene chloride (33 mL) with 33 mL of trifluoroacetic acid. After stirring under argon at room temperature for 2 h, the reaction mixture was washed with brine before being dried over magnesium sulfate. The solvent was evaporated under reduced pressure, and the crude product was purified by gradient column chromatography on silica gel with 0−1% methanol in chloroform. The product was collected by precipitation from a methylene chloride solution into methanol to yield **VII** (1.7 g, 98%). ^{1}H NMR spectral data (400 MHz, $CDCl_3$): δ 1.21 (d, 6H, $-CH_3$), 2.56 (m, 2H, $-CH_2CH(CH_3)CH_2-$), 4.08 (d, 4H, $-CH_2OAr$), 4.47 (m, 4H, $-COOCH_2-$), 6.99 (d, 4H, aromatics), 7.29 (d, 4H, aromatics), 7.60 (d, 4H, aromatics), 7.66 (d, 4H, aromatics), 7.72 (d, 4H, aromatics), 8.14 (d, 4H, aromatics), 8.90 (d, 3H, aromatics).

1,3,5-Benzenetricarboxylic Acid, 1,3-bis[(*R*)-3-[4-[(4′-Cyanobiphenyl-4-yl)oxycarbonyl] phenoxy]-2-methylpropyl] Ester 5-[3-[4-[(4′-Cyanobiphenyl-4-yl)oxycarbonyl]phenoxy]-propyl] Ester, VIII. To a solution of **VII** (0.25 g, 0.26 mmol), 4-(3-hydroxypropoxy)benzoic acid 4′-cyanobiphenyl-4-yl ester ($Nm-OH$, 0.11 g, 0.29 mmol), and TPP (0.076 g, 0.29 mmol) in anhydrous tetrahydrofuran (7 mL) was added DEADC (0.050 g, 0.29 mmol) dropwise. The reaction solution was stirred under argon at room temperature overnight. The solvent was removed under reduced pressure and the crude product was purified by gradient column chromatography with 0−2% acetone in methylene chloride. The product was collected by precipitation from a methylene chloride solution into methanol to yield **VIII** (0.27 g, 79%). Anal. Calcd: C, 73.67; H, 4.71; N, 3.22. Found: C, 73.79; H, 4.59; N, 3.22. ^{1}H NMR spectral data (400 MHz, $CDCl_3$): δ 1.21 (d, 6H, $-CH_3$), 2.34 (quintet, 2H, $-CH_2CH_2CH_2-$), 2.56 (m, 2H, $-CH_2CH(CH_3)-CH_2-$), 4.07 (d, 4H, $-CH_2OAr$), 4.22 (t, 2H, $-CH_2OAr$), 4.47 (m, 4H, $-COOCH_2-$), 4.62 (t, 2H, $-COOCH_2-$), 6.98 (d, 6H, aromatics), 7.29 (d, 6H, aromatics), 7.62 (d, 6H, aromatics), 7.66 (d, 6H, aromatics), 7.72 (d, 6H, aromatics), 8.14 (d, 6H, aromatics), 8.85 (s, 3H, aromatics)

Poly[[7-[4-(3-maleimidopropoxy)benzoyloxy]coumarin]-co-[7-[4-[3-[2-norbornene carbonyloxy]propoxy]benzolyoxy]coumarin]], polymer C. In degassed anhydrous *N,N*-dimethylformamide (3 mL) were dissolved **6** (0.55 g, 1.3 mmol), **7** (0.6 g, 1.3 mmol), and 2,2-azobisisobutyronitrile (0.014 g, 0.087 mmol). After being stirred at 65 °C for 40 h, the reaction mixture was poured into methanol to precipitate polymer **C**. The polymer product was further purified by precipitation twice more from chloroform solution into acetone (0.32 g, 28%). The copolymer composition, **6/7** = 78/22 by mole, was determined by a combination of elemental analysis and ^{1}H NMR spectral data. Anal. Calcd: C, 66.94; H, 4.37.; N, 2.55. Found: C, 66.44; H, 4.46; N, 2.36. ^{1}H NMR spectral data (400 MHz, $CDCl_3$): δ 1.24−3.30 (polymer backbone and $-CH_2CH_2CH_2-$), 3.42−4.19 ($-COOCH_2-$ and $-CH_2OAr-$), 6.36 ($-HC=CHCO-$, coumarin), 6.69−7.10 (aromatics and coumarin), 7.46 (coumarin), 7.66 ($-HC=CHCO-$, coumarin), 8.00 (aromatics).

Molecular Structures and Thermotropic Properties. Molecular structures were elucidated with ^{1}H NMR spectroscopy in $CDCl_3$ or DMSO-d_6 (Avance-400, 400 MHz) and elemental analysis (Quantitative Technologies, Inc.). Thermal transition temperatures were determined by differential scanning calorimetry (DSC, Perkin-Elmer DSC-7) with a continuous N_2 purge at 20 mL/min. Samples were preheated to the to the isotropic state followed by cooling at −20 °C/min to −30 °C, furnishing the reported second heating and cooling scans. Liquid crystalline mesomorphism was character-

ized by hot stage polarizing optical microscopy (DMLM, Leica, FP90 central processor and FP82 hot stage, Mettler, Toledo).

Mechanical Alignment of Glassy GLC Films on Rubbed Polyimide Coatings. Optically flat fused-silica substrates (25.4 mm diameter × 3 mm thickness, Esco Products; $n = 1.459$ at 589.0 nm) were spin-coated with a polyimide alignment layer (Nissan SUNEVER) and uniaxially rubbed. Cholesteric GLC films of **II** through **IV** and **VIII** were prepared between two surface-treated substrates with the film thickness defined by glass fiber spacers (EM Industries, Inc.). Upon melting a powdered cholesteric GLC sample, the fluid film was cooled to $0.77T_c$, where shearing was applied to induce alignment, followed by annealing for 0.5 h. The films were then cooled at −10 °C/h to $0.74T_c$, where additional annealing was performed for 3 h before quenching to room temperature. Transmittance at normal incidence and reflection at 6° off normal were measured with unpolarized incident light using a UV−vis−NIR spectrophotometer (Lambda-900, Perkin-Elmer equipped with a beam depolarizer). Fresnel reflections from the air-glass interfaces were accounted for with a reference cell containing an index-matching fluid ($n = 1.500$ at 589.6 nm) between two surface-treated fused silica substrates. A combination of a linear polarizer (HNP′B, Polaroid) and zero-order quarter waveplate (AO15Z1/4-425, Tower Optical Corporation. or NQM-100-738, Meadowlark Optics, respectively) was employed to produce left- or right-handed circularly polarized light.

Photoalignment of Cholesteric GLC Films. Films of polymers **A**, **B**, and **C** were deposited on optically flat fused-silica substrates transparent to 200 nm (Esco Products) by spin coating from 0.1 wt % chloroform solutions. Linearly polarized irradiation was performed under argon using a 500 W Hg−Xe lamp (model 66142, Oriel) equipped with a dichroic mirror that reflects the light between 260 and 320 nm (model 66217, Oriel), a filter (model 87031, Oriel) that cuts off wavelengths below 300 nm, and a polarizing beam splitter (HPB-308 nm, Lambda Research Optics, Inc.). Polymer **A**, **B**, and **C** films were irradiated at 120, 160, and 196 °C, respectively, corresponding to 1.15 of their respective T_g values. The irradiation intensity was monitored by a UVX digital radiometer coupled with a UVX-31 sensor (UVP, Inc.). The resultant films were characterized with variable angle spectroscopic ellipsometry (V-Vase, J. A. Woollam Corporation) for film thickness and with UV−vis−NIR spectrophotometry (Lambda-900, Perkin-Elmer) for the extent of coumarin dimerization. The insolubility of irradiated films was tested by UV−Vis absorbance after rinsing with chloroform. Cholesteric GLC films of **III** were prepared between photoalignment coatings with the same thermal treatment as described above for mechanical alignment.

Results and Discussion

All the compounds synthesized for this study as shown in Chart 1 were synthesized following the reaction in Scheme 1. To afford hybrid chiral-nematic molecules for the construction of cholesteric GLCs, *Ch*$_1$−OH and *Ch*$_2$−OH were synthesized and characterized as cholesteric liquid crystals. With a more extended rigid rod, *Ch*$_2$−OH exhibits a much wider liquid crystalline temperature range than *Ch*$_1$−OH, as indicated by the DSC thermograms compiled in Figure 1, but both *Ch*$_1$−OH and *Ch*$_2$−OH are prone to crystallization on heating and cooling. The cholesteric mesophase temperature ranges for all the thermograms in Figure 1 were identified by the oily streaks or finger prints observed in situ under polarizing optical microscopy, as shown in the Supporting Information. The tendency of a liquid crystal to crystallize can be overcome by chemical bonding to a

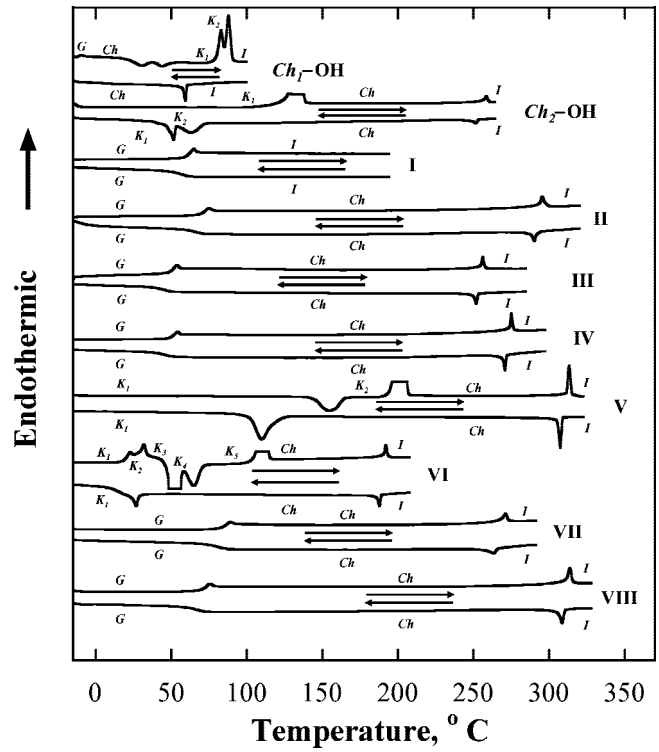

Figure 1. Differential scanning calorimetric heating and cooling scans of *Ch*$_1$−OH, *Ch*$_2$−OH, and **I**−**VIII** at 20 °C/min of samples preheated to beyond clearing points followed by cooling to −30 °C. Symbols: *G*, glassy; *K*, crystalline; *Ch*, cholesteric; *I*, isotropic.

volume-excluding core.[29] Compounds **I** and **II** represent 1,3,5-trisubstitution on a benzene core. Although both *Ch*$_1$−OH and *Ch*$_2$−OH are morphologically unstable cholesteric liquid crystals, **I** is an amorphous solid with a T_g at 63 °C, and **II** is a morphologically stable cholesteric GLC with a T_g at 73 °C and a T_c at 295 °C. The morphologies of Compounds **I** and **II** suggest that the hierarchy in molecular order is lowered by attaching *Ch*$_1$−OH and *Ch*$_2$−OH to a benzene core. To the best of our knowledge, **II** is the first cholesteric GLC comprising hybrid chiral-nematic pendants bonded to a volume-excluding core via a chiral spacer. A prior attempt using a chiral spacer between cyanotolan and a cyclohexane ring resulted in an amorphous material.[21] Other attempts at benzene and cyclohexane cores with pendants incorporating a chiral tail to a nematic segment yielded exclusively smectic mesomorphism.[40]

Compounds **III**, **IV**, **V**, and **VI** serve to elucidate how the number of hybrid chiral-nematic pendants and regiosiomerism affect solid morphology, phase-transition temperatures, and selective reflection property. The DSC thermograms shown in Figure 1 indicate that with ortho- and meta-isomers on a benzene core, **III** and **IV** form morphologically stable cholesteric GLCs with the same T_g, whereas **IV** exhibits a T_c about 20 °C higher than that of **III**. In contrast, para-disubstitution and monosubstitution, as in **V** and **VI**, result in cholesteric liquid crystals that crystallize on heating and cooling without evidence of glass transition. Nevertheless, para-disubstitution is responsible for the highest T_c of all with monosubstitution lagging behind all others by 60 to 120 °C. Our prior approach to cholesteric GLCs incorporating separate chiral and nematic pendants[22,26,36−39] is revisited here with Compounds **VIII** and its precursor **VII**, both found

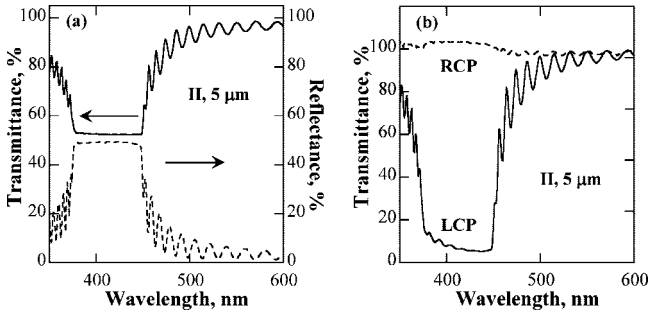

Figure 2. (a) Transmission and reflection spectra with unpolarized incident light and (b) circularly polarized transmission spectra of a 5 μm thick cholesteric GLC film of **II** between rubbed polyimide films.

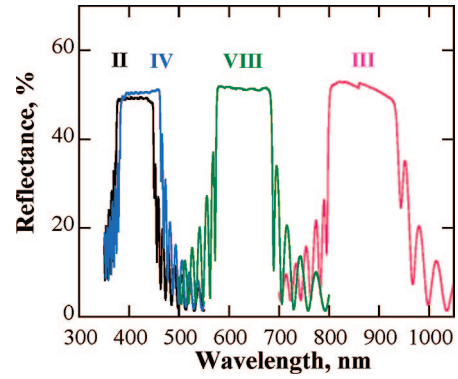

Figure 3. Reflection spectra of cholesteric GLC films of **II**, **III**, **IV**, and **VIII** with unpolarized incident light.

to be morphologically stable cholesteric GLCs. Because of intermolecular hydrogen bonding involving carboxylic acid groups, Compound **VII** shows a T_g 35 °C higher than **IV** but with little difference in T_c between the two. For the same 1,3,5-trisubstitution on a benzene core, **VIII** exhibits about 20 °C elevation in T_c over **II** with no difference in T_g between the two. A comparison of the phase transition temperatures of all morphologically stable glassy liquid crystals leads to a conclusion that both T_g and T_c increase with the number of hybrid chiral-nematic mesogens to a single benzene core.

To characterize the selective wavelength reflection property of cholesteric liquid crystals,[46,47] we prepared monodomain cholesteric GLC films between rubbed polyimide films as described in the Experimental Section for the measurement of transmittance and reflectance. The results are illustrated in Figure 2a with a 5 μm thick film of **II**, showing a selective reflection band centering at $\lambda_R = 413$ nm. Figure 2b presents the transmission of right-handed circularly polarized light and the reflection of the left-handed counterpart, indicating a left-handed helical stack of quasi-nematic layers with (*S*)-3-bromo-2-methylpropanol as the chiral precursor.

With (*S*)-3-bromo-2-methylpropanol as the chiral building block, left handedness was identified for films prepared with all the compounds reported herein. A right-handed helical stack is expected of (*R*)-3-bromo-2-methylpropanol as the chiral precursor with the same λ_R. A mixture of these two enantiomeric cholesteric GLCs at varying ratios will generate films with λ_R ranging continuously from blue, through the visible to infrared region, ultimately reaching an infinite λ_R with an equimolar mixture.

The selective reflection spectra of 5 μm thick morphologically stable cholesteric GLC films **II**, **III**, **IV**, and **VIII** are presented in Figure 3. With the hybrid chiral-nematic mesogens on a benzene core at 1,3,5- and 1,3-positions, respectively, cholesteric GLC films of **II** and **IV** have nearly the same selective reflection wavelength, λ_R, at 413 versus 422 nm. In contrast, the cholesteric GLC film of **III** with a 1,2-disubstitution has a much longer λ_R at 860 nm. With two hybrid chiral-nematic mesogens and one nematic mesogen to a benzene core, the cholesteric GLC film of **VIII** has its λ_R at 630 nm, which is still shorter than **III** despite the dilution by a nonchiral nematogen per molecule, further evidence that regioisomerism plays an important role in selective reflection property despite the dilution by a nematic mesogen compared to **III**.

Molecular packing involving chiral moieties was recognized as an origin of the difference in helical twisting and hence λ_R. The Gaussian 2003 software package was employed to compute molecular geometries using B3LYP functionals with the 6−31G(d) basis set. Because of the number of atoms involved, computations were limited to single molecules. Instead of the entire molecules of **III** and **IV**, the portions from the benzene core to chiral spacers were computed since the rest of the rigid pendants are linear, viz. irrelevant to the depiction of molecular packing in relation to helical twisting. Limiting the number of atoms per molecule is also advantageous to computation time and accuracy. Structures a and b in Figure 4 reveal the top- and side-views of the ortho-isomer, and panels c and d those of the meta-isomer, respectively. It is evident that oxygen atoms are twisted out of plane defined by the benzene core in the ortho-isomer because of steric hindrance. The nonplanar geometry restricts the two chiral moieties to acting independently. In contrast, the meta-isomer has a rather planar geometry, permitting the two chiral moieties to act in unison. This difference in molecular geometry and the resulting packing behavior seems to be responsible for the shorter λ_R in the meta-isomer than the ortho-isomer. Following this line of argument, cholesteric GLC films of **II** and **IV** should have comparable λ_R values, as borne out in Figure 3.

Traditionally, cholesteric liquid crystalline films are oriented on rubbed polyimide films to yield both reflectance and transmittance approaching the theoretical limit of 50%.[46,47] Although coumarin-containing polymer films are capable of photoalignment of a nematic fluid (i.e., E-7) and glassy-nematic oligofluorene films,[41−45,48,49] the orientation of helically stacked cholesteric glassy liquid crystalline films have not been attempted thus far. Compound **III** was used here to test the amenability of cholesteric GLCs to photoalignment on films of polymers **A**, **B**, and **C** as depicted in

(46) de Gennes, P. G. *The Physics of Liquid Crystals*; Oxford University Press: Oxford, U.K., 1974; p 216.
(47) Chandrasekhar, S. *Liquid Crystals*; Cambridge University Press: Cambridge, U.K., 1992; p 213.
(48) Trajkovska, A.; Kim, C.; Marshall, K. L.; Mourey, T. H.; Chen, S. H. *Macromolecules* **2006**, *39*, 6983.
(49) Kim, C.; Wallace, J. U.; Chen, S. H.; Merkel, P. B. *Macromolecules* **2008**, *41*, 3075.

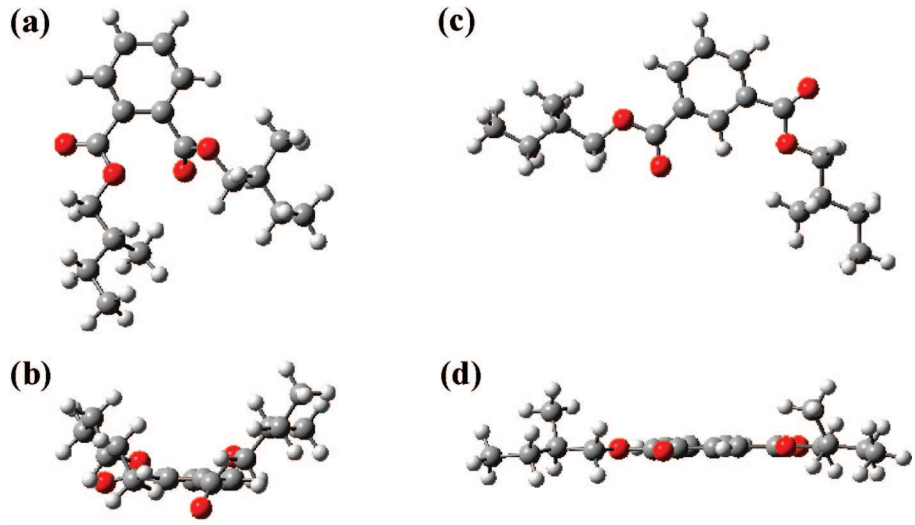

Figure 4. Computed structures of the moieties from benzene core to chiral spacers for **III**, (a, b) with ortho-disubstitution; and for **IV** and (c, d) with meta-disubstitution.

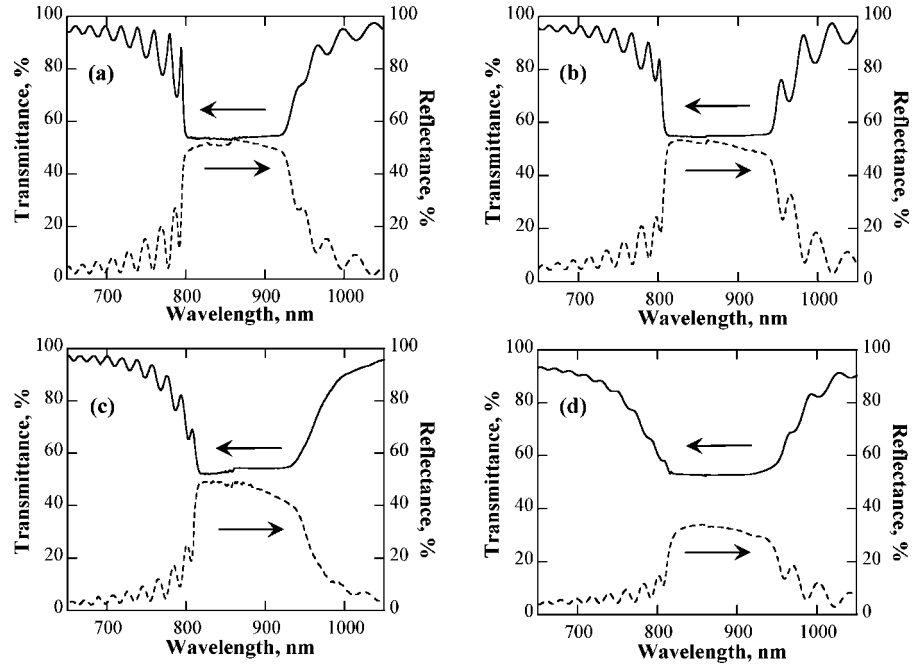

Figure 5. Transmission and reflection spectra of cholesteric GLC film of 7 μm thick films of **III** sandwiched between (a) rubbed polyimide films; (b) polymer **A** films irradiated with 0.2 J/cm^2 at 120 °C to $X = 0.24$; (c) polymer **B** films irradiated with 0.5 J/cm^2 at 160 °C to $X = 0.24$; and (d) polymer **C** films irradiated with 0.5 J/cm^2 at 196 °C to $X = 0.27$.

Chart 2. Polymers **A** and **B** had been synthesized and characterized previously,[44] and polymer **C** was synthesized following the reaction in Scheme 2.

Polymer **C** has a higher T_g than polymers **A** and **B**, 135 versus 102 and 68 °C, respectively. Spin-cast films of polymers **A**, **B**, and **C** were irradiated with linearly polarized light at 300−320 nm to effect coumarin dimerization preferentially along the polarization axis of irradiation. Polarized UV-irradiation was conducted at $1.15T_g$ with a fluence of 0.2 J/cm^2 for polymer **A** and 0.5 J/cm^2 for polymers **B** and **C**. The extents of coumarin dimerization, X, were determined by UV−vis absorption spectroscopy[45] at 0.24, 0.24, and 0.27 for polymers **A**, **B**, and**C**, respectively, sufficient to ensure film insolubility in chloroform. Pairs of fused silica substrates with the resultant UV-irradiated polymer films and rubbed polyimide films were used to prepare 7 μm thick cholesteric GLC films of **III** via thermal annealing with subsequent cooling to room temperature.

As shown in panels a and b Figure 5, the transmission and selective reflection spectra of a 7 μm thick film of **III** sandwiched between photoalignment films prepared with polymer **A** are close to those for a film between uniaxially rubbed polyimide films, the traditional approach to liquid crystal orientation. Polymer **B** is slightly inferior in its ability to orient **III** than polymer **A** because of the shorter flexible spacer to the same methacrylate backbone, panel c compared to panel b in Figure 5. Because of the more rigid and bulky backbone with a propylene spacer to coumarin monomers, polymer **C** films fall short of their capability for photoalig-

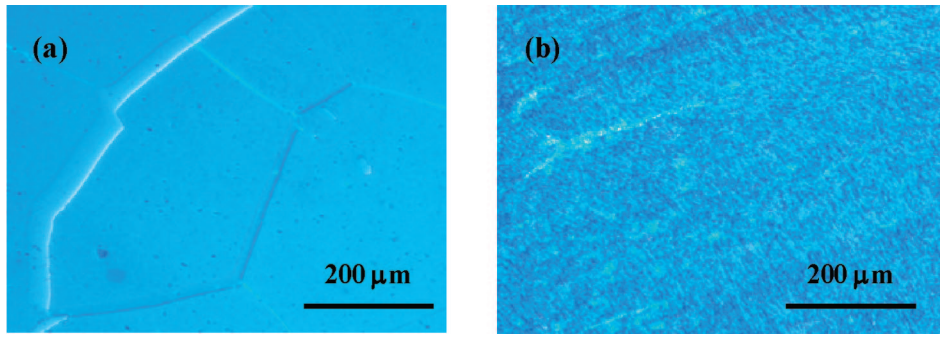

Figure 6. Polarizing optical micrographs of 7 μm thick cholesteric GLC films of **III** sandwiched between (a) polymer **A** films irradiated with 0.2 J/cm^2 at 120 °C to $X = 0.24$; and (d) polymer **C** films irradiated with 0.5 J/cm^2 at 196 °C to $X = 0.27$.

ment in comparison to polymers **A** and **B**; see Figure 5d versus panels b and c in Figure 5.

The polarizing optical micrographs presented in Figure 6a indicate that the cholesteric GLC film of **III** between irradiated polymer **A** films consists of large Grandjean domains. In contrast, the cholesteric GLC film of **III** between irradiated polymer **C** films comprises a large number of very small domains, as shown in Figure 6b. Because these small domains have a distributed surface normal, a limited fraction of the diffuse reflection of incident unpolarized light is detected at 6° off normal, see Figure 5d versus Figure 5b. In contrast, the transmittance of the polydomain film is comparable to that of the nearly monodomain film because the transmitted light is right-handed which does not interact with the left-handed Grandjean domain regardless of its size and orientation. Nevertheless, the small domains in **III** between polymer **C** films may scatter incident light, causing the shallow edges of the transmission spectrum shown in Figure 5d.

Irradiation of the coumarin-containing polymer films of polymers **A**, **B**, and **C** at the same temperatures relative to their respective T_g value permits a sensible comparison of their photoalignment behaviors in terms of the rotational mobility of pendant coumarin monomers relative to the polarization axis of irradiation. The longer spacer in polymer **A** imparts a higher mobility on coumarin monomers than that in polymer **B**. The more rigid and bulky backbone in polymer **C** than polymers **A** and **B** could also restrict mobility of pendant coumarin monomers. The more mobile coumarin monomers in polymer **A** than in polymer **B** are more reactive toward polarized irradiation thanks to reaction-induced molecular rotation, thus requiring less fluence to dimerize to the same extent with better oriented coumarin dimers along the polarization axis of UV-irradiation. The more abundant and better oriented coumarin dimers also contributed to the better photoalignment capability of polymer **A** than polymer **B** for a glassy-nematic pentafluorene.[44] These results suggest the important roles played by rotational mobility of pendant coumarin monomers, as affected by the polymer backbone rigidity and the flexible spacer length, in the outcome of photoalignment of cholesteric GLCs.

Conclusions

Novel cholesteric GLCs were successfully developed using 4′-cyanobiphenyl-4-yl benzoate nematogens and enantiomeric 2-methylpropylene spacers to a benzene core. A systematic investigation was conducted for mesomorphic behavior, morphological stability, and optical properties in relation to the extent of substitution and regioisomerism. Amenability to photoalignment on coumarin-containing polymer films was also tested with a morphologically stable cholesteric GLC. Key findings are recapitulated as follows:

(1) Glass-forming ability generally improves with an increasing substitution with hybrid chiral-nematic mesogens on the benzene ring. Of all the cholesteric liquid crystals reported here, the para-disubstituted and the monosubstituted systems lack glass-forming ability. With T_g at 73 °C and T_c at 295 °C, the 1,3,5-trisubstituted system is the most preferable of all. Left at room temperature for months, the cholesteric GLC films prepared with meta- and ortho-isomers in addition to 1,3,5-trisubstituted system have remained noncrystalline, evidence of superior morphological stability.

(2) Morphologically stable cholesteric GLC films were characterized for their selective reflection properties. Left-handed helical stacking emerged with (*S*)-3-bromo-2-methylpropanol as the chiral precursor. Films of the 1,3,5-trisubstituted and meta-disubstituted systems show a λ_R at 413 and 422 nm, respectively, whereas that of the ortho-isomer system exhibits a λ_R at 860 nm. Replacing one of the hybrid chiral-nematic mesogens in the 1,3,5-trisubstituted system by a nematogen loosens the helical pitch to yield a λ_R at 630 nm, still shorter than the ortho-isomer despite the dilution by nematogen. Compared to the ortho-isomer, the greater helical twisting exhibited by the meta-isomer was attributed to planar geometry from the benzene core to the chiral spacer, permitting the two chiral moieties to act in unison.

(3) The ortho-isomer is amenable to photoalignment on films of methacrylate homopolymers and a maleimide-norbornene copolymer containing pendant coumarin monomers to a varying extent. With an extent of coumarin dimerization to about 0.25 as a result of linearly polarized UV-irradiation, the films of a methacrylate polymer with a hexamethylene spacer produced a 7 μm thick monodomain cholesteric GLC film with selective reflection properties equivalent to mechanical alignment on rubbed polyimide films. In contrast, the rigid and bulky polymer backbone and the short flexible spacer in the maleimide-norbornene copolymer produced a polydomain cholesteric GLC film with inferior selective reflection characteristics. These observations

were interpreted by the rotational mobility of pendant coumarin monomers relative to the polarization axis of irradiation.

Acknowledgment. The authors thank Stephen D. Jacobs of the Laboratory for Laser Energetics, LLE, at University of Rochester for helpful discussions and technical advice. They are grateful for the financial support provided by Eastman Kodak Company, and the New York State Center for Electronic Imaging Systems. J.U.W. acknowledges the support of a Horton Graduate Fellowship administered by the LLE. Additional funding was provided by the Department of Energy Office of Inertial Confinement Fusion under Cooperative Agreement DE-FC52-08NA28302 with LLE and the New York State Energy Research and Development Authority. The support of DOE does not constitute an endorsement by DOE of the views expressed in this article.

Supporting Information Available: Synthesis, purification and characterization data for intermediates **1**−**7**, and polarizing optical micrographs for identification of cholesteric mesomorphism (PDF). This material is available free of charge via the Internet at http://pubs.acs.org.

CM801623A